Optimal Droop Control of ESS Using Quasi-Static Time-Series Simulation in Islanded Microgrids

Hyeonseong Mun
Korea Electric Power Corporation (KEPCO)
Naju, South Korea

Surya Santoso
The University of Texas at Austin
Austin, TX, USA

***Abstract*—This paper presents an optimal droop control strategy and framework for energy storage systems (ESSs) in islanded microgrids using quasi-static time-series (QSTS) simulation. In the absence of a slack bus, ESSs should autonomously regulate frequency and voltage while maintaining state-of-charge (SoC) over extended operation. To address these challenges, the proposed framework integrates droop-based power sharing, SoC-aware dispatch strategies, and multi-norm cost tracking to minimize control effort and enhance system resilience. Five control strategies—uncontrolled baseline, heuristic, rule-based, hybrid, and adaptive—are evaluated under identical conditions. Simulation results represent that the adaptive strategy achieves superior frequency stability and SoC preservation with minimal control effort, extending microgrid operability by approximately 7% compared to the baseline under variable load and PV generation conditions. The proposed framework and strategy enable systematic design of ESS droop control policies, enhancing stability and sustainability in islanded microgrids.**

***Index Terms*—Islanded microgrids, energy storage system (ESS), droop control, optimal control, quasi-static time-series (QSTS) simulation, adaptive control, state-of-charge (SoC) management.**

I. Introduction

Energy storage systems (ESSs) are increasingly deployed in islanded microgrids to improve reliability, power quality, and operational autonomy, with particular significance for remote communities and critical infrastructure [1]–[4]. Unlike grid-connected systems, islanded microgrids lack a centralized slack bus to maintain frequency and voltage, requiring distributed energy resources (DERs) to autonomously coordinate power balance. This makes ESS control both essential and challenging, as it is required to maintain stable operation over long durations, variable loads, and fluctuating renewable generation [5], [6].

A primary challenge in islanded microgrids is the concurrent regulation of voltage and frequency while maintaining the state-of-charge (SoC) of the ESS, as these objectives frequently conflict under prolonged disturbances or limited renewable generation. Conventional AC steady-state power flow simulation tools are not well-suited to represent the slow time-scale evolution and energy-constrained operation arising in such conditions. To address this gap, this paper proposes an optimal ESS droop control framework using quasi-static time-series (QSTS) simulation. The proposed framework represents time-varying load, solar generation, and SoC through sequential AC steady-state power flow calculations, implemented through MATLAB–OpenDSS integration to ensure accurate AC power flow analysis and flexible control execution at each time step.

Dynamic droop adjustment has been increasingly adopted to improve energy storage utilization and maintain system balance in microgrids [7]. In this study, five ESS droop control strategies are evaluated under identical operating conditions: (1) a control-free (baseline), (2) a heuristic approach based on frequency or SoC constraints, (3) a rule-based method that automates the heuristic rules, (4) a hybrid scheme combining (2) and (3), and (5) an adaptive strategy that dynamically responds to real-time measurements. These strategies collectively enable a structured assessment of ESS control performance, offering insights into robust design for islanded microgrids.

II. Theoretical Background

This section outlines the theoretical foundations for simulating islanded microgrids. It addresses the QSTS simulation methodology, inverter classifications, droop control principles, frequency estimation, and the operational characteristics and SoC dynamics of ESS under these conditions.

A. Quasi-Static Time-Series Simulation

QSTS simulation is a time-domain approach for representing the slow time-scale dynamics of power systems by sequentially solving AC steady-state power flow problems at fixed intervals Δt [8]. It effectively captures long-term variations in load demand, solar irradiance, and SoC without the computational burden associated with electromagnetic transient simulations. In this work, QSTS is implemented using a MATLAB–OpenDSS co-simulation framework, where MATLAB executes the control algorithms to compute ESS real-power setpoints, and OpenDSS solves the corresponding AC power flow, with solution convergence determined internally by the solver. The resulting voltage, current, and active/reactive power flow data are then returned to MATLAB for SoC updating and subsequent control actions. This architecture enables flexible, high-resolution assessment of droop-based and alternative ESS control strategies under realistic, time-varying operating conditions.

B. Inverter Classification by Functionality

In modern microgrid power systems, inverters are generally classified into the following four categories based on their functionality and control strategy. This classification defines how each inverter interacts with the grid [9].

- **Grid-feeding inverters**: Operate as current sources synchronized with the grid, delivering specified active and reactive power. They cannot establish voltage or frequency.

979-8-3315-8138-1

- **Grid-forming inverters**: This inverter actively regulates the system frequency and voltage level at the point of connection (POC). It should be coupled with a reliable power source, such as an ESS, to act as a stable reference.
- **Current-source-based grid-supporting inverters**: These inverters regulate their output current according to droop characteristics, contributing to voltage and frequency support. Their operation requires the presence of a reference voltage provided by at least one grid-forming unit.
- **Voltage-source-based grid-supporting inverters**: Function as voltage sources employing droop characteristics, thereby contributing to autonomous frequency and voltage regulation in the absence of communication links.

Within microgrid operation, understanding these roles is essential. In particular, Grid-supporting inverters—both current- and voltage-source-based—are fundamental to decentralized control and the stability of islanded microgrids.

C. Droop Control for Distributed Inverters

Droop control regulates the output of the inverter based on local measurements of frequency and voltage, emulating the behavior of synchronous generators [10]. It enables decentralized power sharing among DERs without real-time communication. The standard droop equations are:

$$\omega = \omega_0 - m_p(P - P_0), \quad V = V_0 - n_q(Q - Q_0) \tag{1}$$

where ω_0 and V_0 denote the nominal frequency and voltage, P_0 and Q_0 are the power setpoints, and m_p and n_q represent the droop slopes for active and reactive power, respectively [8]. Smaller slopes provide tighter frequency and voltage regulation but may compromise sharing accuracy, whereas larger slopes enhance proportionality at the expense of deviations. The slopes are calculated from inverter ratings and allowable limits as

$$m_p = \frac{\omega_{\max} - \omega_{\min}}{P_{\text{nom}}}, \quad n_q = \frac{V_{\max} - V_{\min}}{Q_{\text{nom}}} \tag{2}$$

In practical implementations, the droop response is modified by a resource availability scaling factor $\text{shape}_{\text{dis}} \in [0, 1]$ that reflects the instantaneous availability of distributed resources (e.g., ESS SoC or PV irradiance). With ω_{ref} and V_{ref} as local references, the resulting droop equations are [8]:

$$P = P_0 - \frac{\text{shape}_{\text{dis}}}{m_p}(\omega - \omega_{\text{ref}}), \quad Q = Q_0 - \frac{1}{n_q}(V - V_{\text{ref}}) \tag{3}$$

This formulation enables resource-aware power dispatch while preserving decentralized stability.

D. Frequency Estimation Under Distributed Droop Control

Unlike conventional power flow analysis, which assumes a fixed nominal frequency (e.g., 50 or 60 Hz) maintained by a slack bus, islanded microgrids must determine system frequency dynamically based on internal power balance. In the absence of an external reference, the frequency evolves according to the aggregate droop response of distributed generators.

At each time step of the QSTS simulation, the operating angular frequency ω is updated using the net real power imbalance and the combined droop characteristics of all grid-forming or grid-supporting sources as [8]:

$$\omega = \omega_{\text{ref}} - \left(\sum_{k \in \{\text{PV, ESS}\}} \frac{\text{shape}_{\text{dis}}^k}{m_p^k} \right)^{-1} P_{\text{change}} \tag{4}$$

where P_{change} denotes the net active power mismatch in the microgrid.

This droop-based frequency adjustment enables decentralized and scalable frequency regulation in islanded microgrids, accounting for heterogeneous generation availability.

E. ESS Operation and SoC Dynamics

In islanded microgrids, ESSs regulate active power and play an essential role in balancing supply and demand. Their operation is limited by the finite capacity of the battery, represented by the SoC. The SoC dynamics are given by:

$$\text{SoC}_{k+1} = \text{SoC}_k + \frac{\eta_{\text{ch}} P_{\text{ch}} - \frac{P_{\text{dis}}}{\eta_{\text{dis}}}}{E_{\text{rated}}} \Delta t \tag{5}$$

where P_{ch} and P_{dis} are the charging and discharging powers, η_{ch} and η_{dis} are their respective efficiencies, and E_{rated} is the energy capacity of the ESS. Accurate SoC tracking is essential to avoid excessive cycling and to prolong battery lifespan.

By integrating QSTS simulation with droop-based inverter control and SoC-aware dispatch, the proposed control strategy aims to ensure both dynamic stability and extended operational lifetime in islanded microgrid operations.

III. Control Strategy

In islanded microgrids, maintaining frequency stability and energy balance is particularly challenging due to the absence of connected-grid and the inherent variability of local resources. This section analyzes the characteristics of various control strategies and introduces those applicable to ESS droop control.

A. Heuristic Control

Heuristic control manually adjusts the ESS droop setpoint according to predefined frequency and SoC limits mainly. For example, when the SoC or frequency deviates above or below a specified threshold, the droop coefficient is modified, relying on simple decision rules based on fixed thresholds. While computationally efficient and easy to implement, this approach has limited adaptability to disturbances and can lead to overly conservative or delayed responses under rapid system changes.

B. Rule-Based Control

Rule-based control extends heuristic logic by employing structured nested conditionals or piecewise mappings to adjust the ESS droop setpoint. It can utilize multiple variables—such as frequency deviation and SoC—either independently or in combination to determine dispatch priority, enabling finer granularity and multi-variable responsiveness within predefined rules. However, similar to heuristic methods, it requires manual tuning, lacks adaptation based on operational feedback, and may induce excessive control actions under critical conditions.

C. Adaptive Control

To address the inherent rigidity of rule-based methods, an adaptive control strategy is employed to continuously adjust the P_0 using real-time feedback [11]–[14]. The controller takes system frequency f, SoC S, and solar irradiance G as inputs, forming $x = [f,\, S,\, G]^\top$. A reference signal is defined as

$$P_{0,\text{ref}} = k_f(f_{\text{ref}} - f) + k_{\text{soc}}(S - S_{\text{ref}}) - k_{\text{irr}}G \tag{6}$$

where k_f, k_{soc}, and k_{irr} are predefined weighting coefficients. This structure penalizes frequency deviations, regulates SoC around its nominal level, and biases charging according to solar availability. The weighting coefficients determine the relative emphasis placed on frequency regulation, energy sustainability, and renewable utilization, thereby shaping the trade-off between dynamic response and control effort. The adaptive output is

$$P_{0,\text{adapt},k} = \theta_k^\top x_k, \qquad \theta_k \in \mathbb{R}^3 \tag{7}$$

and the parameter vector θ is updated at each simulation step by a least-mean-squares (LMS) type gradient rule with projection:

$$\theta_{k+1} = \Pi_\Theta\big(\theta_k + \gamma\, x_k\big(P_{0,\text{ref},k} - P_{0,\text{adapt},k}\big)\big) \tag{8}$$

where $\gamma > 0$ is the learning rate. In the implementation, the projection $\Pi_\Theta(\cdot)$ is realized as element-wise parameter clipping to predefined upper and lower bounds. Output saturation and a small deadband are applied to ensure compliance with hardware limits and eliminate small-signal dithering.

Unlike static droop methods, this adaptive strategy updates the dispatch law in response to operating conditions, thereby enhancing robustness against transient situations and helping to maintain frequency and SoC stability without manual retuning. This state-dependent adaptation mitigates the inherent trade-offs between frequency regulation and SoC management.

IV. Islanded Microgrid

To evaluate the performance of the proposed ESS control strategies, a detailed QSTS simulation environment is implemented in MATLAB co-simulated with OpenDSS. The simulation models a single-phase islanded microgrid equipped with PVs and an ESS operating in grid-forming mode [8].

A. System Configuration

The test microgrid comprises three buses interconnected by two single-phase distribution lines, each hosting local loads. PV units are installed at Buses 2 and 3. In the initial grid-connected mode (Fig. 1), Bus 2 operates as the slack bus via a voltage source, providing stable voltage and power flow references.

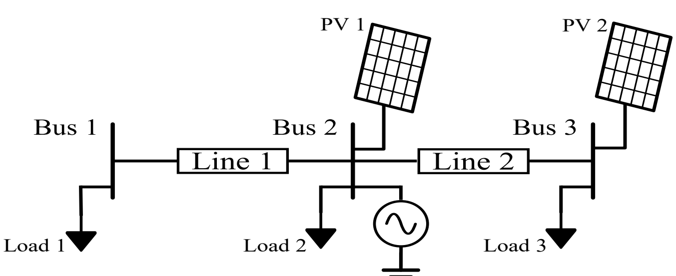

Fig. 1. Microgrid in grid-connected mode

Following disconnection from the main grid, the system transitions to islanded operation with an ESS at Bus 1 acting as a grid-forming unit to supply voltage and frequency references (Fig. 2). The ESS maintains power balance under varying load and PV generation, enabling autonomous microgrid operation. Component specifications and control parameters for the islanded configuration are summarized in Table I.

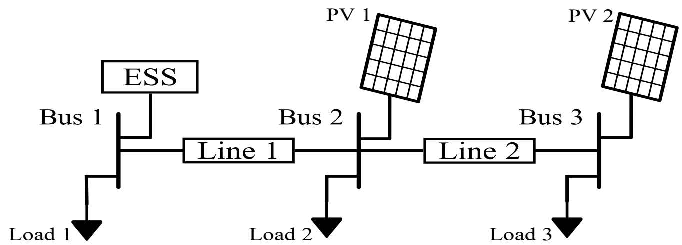

Fig. 2. Microgrid in islanded mode

TABLE I
Islanded Microgrid Configuration Summary

Component	Specifications
Microgrid Overview	
System Voltage	240 V, single-phase
Operating Frequency	56–63 Hz
Topology	3 nodes, 2 distribution lines
Distributed Energy Resources (DERs)	
ESS (Node 1)	
Ratings	240 [V], 10 [kW], 14 [kVA], 28 [kWh]
Voltage Droop Setting	$V_{\max} = 1.05$ [p.u.], $V_{\min} = 0.95$ [p.u.]
Power droop Setpoints	P_0 (variable), $Q_0 = 0$
Frequency Droop Range	$\omega_{\max} = 1.01$ [p.u.], $\omega_{\min} = 0.99$ [p.u.]
PV Resources (Node 2 and 3)	
Ratings	240 [V], 10 [kW], 14 [kVA]
Irradiance	Time-varying profile applied
Voltage Droop Setting	$V_{\max} = 1.05$ [p.u.], $V_{\min} = 0.95$ [p.u.]
Power droop Setpoints	$P_0 = 0$, $Q_0 = 0$
Frequency Droop Range	$\omega_{\max} = 1.01$ [p.u.], $\omega_{\min} = 0.99$ [p.u.]
Loads (at Nodes 1–3)	
PQ Load	240 [V], 5 [kW]
	Time-varying profile applied
Distribution Lines	
Line #1 (1.0 [mi])	r=0.03167, x=0.0158 [Ω/mi]
Line #2 (0.3 [mi])	c=0.5287 [μS/mi]

B. Load and PV Profiles

The simulation spans 24 hours with a 1-minute resolution. Residential demand is scaled from historical data to a 5 kW peak per household, and PV generation is derived from clear-day irradiance with a 10 kW peak. Both profiles are shown in Fig. 3 in normalized form, highlighting their daily variation. The time series are interpolated to match the QSTS timestep.

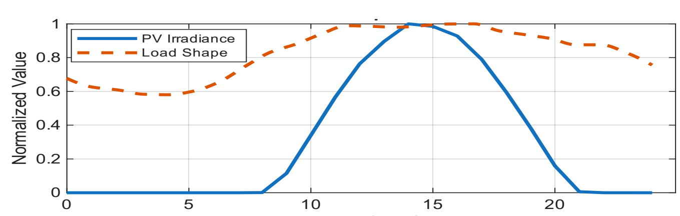

Fig. 3. Normalized load and PV profiles over 24 hours

V. Simulation Setup

This section describes the QSTS-based simulation used to compare ESS control strategies in an islanded microgrid.

A. QSTS Simulation Framework

The QSTS framework discretizes the simulation into minute-scale intervals. The microgrid is first initialized in grid-connected mode with a slack/swing bus to establish voltage and angle references. The slack bus is then disabled, and the ESS is configured for grid-forming operation to provide references.

At each timestep $t_k = k\,\Delta t$, MATLAB updates load $P_{\mathrm{L}}(t_k)$, irradiance $G(t_k)$, and the ESS droop setpoint $P_0(t_k)$, which are transferred to OpenDSS for a single-phase AC power-flow solution with DER models. Upon convergence, MATLAB retrieves the nodal voltage V and updates the active and reactive power setpoints, adjusting the PV and ESS outputs accordingly. This co-simulation framework integrates MATLAB-based control logic with OpenDSS's solver to capture long-term dynamics in islanded microgrids [8].

The simulation then proceeds by repeating the following steps for each timestep:

1) Update load and PV profiles from the database.
2) Execute control logic (e.g., adaptive control) to determine the ESS droop setpoint P_0.
3) Adjust system frequency using droop equations.
4) Solve AC steady-state power flow in OpenDSS.
5) Update ESS SoC and enforce operational constraints.

The simulation is terminated when the frequency exceeds the range of 56–63 Hz, the SoC falls outside the 0–100% range, or the voltage magnitude lies outside 0.95–1.05 p.u.. Throughout the simulation, the framework records frequency, voltage, SoC, and control effort for quantitative comparison of the strategies.

B. Control Strategy Design

Five ESS control strategies are evaluated within the QSTS simulation framework. Case 1 is a control-free (*Baseline*) for comparison. Case 2 (*Heuristic Control*) applies threshold-based logic. Case 3 (*Rule-Based Control*) employs structured conditional rules. Case 4 (*Hybrid Control*) combines the condition-based logic of Case 2 with the structured decision-making of Case 3, switching between them based on the operating context to improve flexibility. Case 5 (*Adaptive Control*) updates P_0 in real time using system feedback.

All strategies are implemented in the QSTS environment to enable direct comparison of operational performance, control effort, and energy sustainability under identical conditions.

C. Performance Evaluation Metrics

Control performance is evaluated using three metrics: (1) frequency and voltage deviations over the simulation horizon, (2) the ESS SoC trajectory to assess operational sustainability, and (3) normalized 1-norm and squared 2-norm control efforts, defined as

$$\bar{J}_1 = \frac{1}{T}\sum_k \left|P_{0,k} - P_{0,k-1}\right|, \quad \bar{J}_2 = \frac{1}{T}\sum_k \left(P_{0,k} - P_{0,k-1}\right)^2 \tag{9}$$

VI. Results

This section presents the simulation results for the different control strategies. The performance of each strategy is evaluated in terms of simulation sustainability, frequency and voltage stability, ESS variations, and droop control cost, under identical conditions within the proposed QSTS framework using a MATLAB–OpenDSS co-simulation environment.

A. Simulation Duration and Robustness

The simulation was performed with a 1-minute resolution starting at 00:00, and the control strategies were activated at 07:00 to represent a full daily cycle. Simulations were terminated upon violation of operational constraints, such as frequency or SoC limits. As summarized in Table II, all cases eventually terminated due to under-frequency violations. The baseline (Case 1) ended at 20:47, corresponding to 81.1% of the simulated period. Among the controlled cases, the rule-based strategy (Case 3) yielded the shortest duration, ending at 21:40 (86.3%), whereas the heuristic (Case 2) and hybrid (Case 4) strategies extended operation until 21:47 (87.0%) and 21:49 (87.2%), respectively. The adaptive controller (Case 5) achieved the longest survivability, operating until 21:59 (88.1%), thereby demonstrating enhanced robustness under adverse conditions.

TABLE II
Survivable Operation Duration Across Five Cases

Case	Control Strategy	Simulation End	Violation
1	Baseline	20:47 (81.1%)	Under-frequency
2	Heuristic	21:47 (87.0%)	Under-frequency
3	Rule-based	21:40 (86.3%)	Under-frequency
4	Hybrid	21:49 (87.2%)	Under-frequency
5	Adaptive	21:59 (88.1%)	Under-frequency

B. Frequency and Voltage Stability

All five strategies successfully maintained voltage within the prescribed 0.95–1.05 p.u. range. However, their frequency profiles exhibited distinct behaviors. As illustrated in Fig. 4, the heuristic and rule-based controllers showed significant frequency deviations in response to rapid load fluctuations, occasionally nearing violation thresholds. In contrast, the adaptive strategy maintained a notably smoother frequency response, enabling uninterrupted operation. This smoother response arises from state-dependent adjustment of control action, rather than reliance on fixed control gains. These results highlight that feedback-driven control strategies are effective at damping frequency excursions under dynamic conditions.

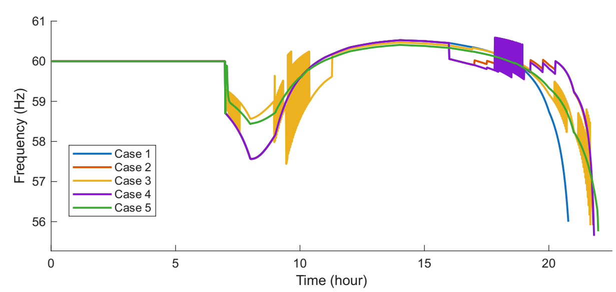

Fig. 4. Frequency trajectories under different ESS control strategies

979-8-3315-8138-1

C. ESS SOC Trajectory

The SoC evolution is shown in Fig. 5. The adaptive control strategy (Case 5) smooths SoC utilization, resulting in a balanced SoC profile. In contrast, Cases 2–4 respond more reactively and discharge the ESS aggressively, leading to faster depletion and earlier ESS runout under high-demand scenarios.

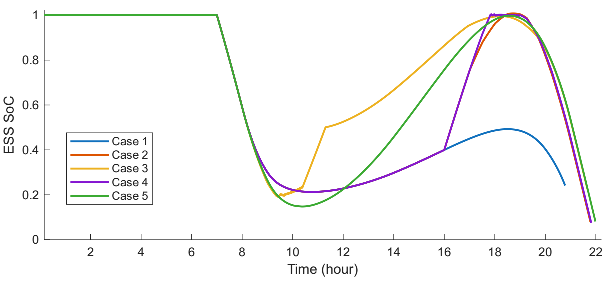

Fig. 5. SoC trajectories under different ESS control strategies

D. ESS Power Output and Cost Metrics

The ESS droop setpoint exhibited smoother transitions under adaptive control compared to other strategies, reducing abrupt changes and associated control effort. As shown in Fig. 6, heuristic and rule-based controllers caused large step variations, resulting in significantly higher 1-norm and 2-norm cost values.

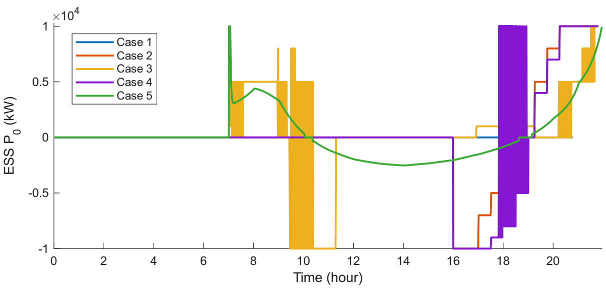

Fig. 6. Droop setting trajectories under different ESS control strategies

Table III summarizes the control effort associated with each strategy. The adaptive control strategy achieved one of the lowest costs, demonstrating substantially better performance than Cases 3–4. In rule-based control approaches, frequent oscillations around the threshold led to sharp increases in control effort, leading to significantly higher costs. The baseline case incurred zero cost but offered no dynamic regulation.

TABLE III
ESS CONTROL COST COMPARISON ACROSS FIVE CASES

Case	Control Strategy	1-norm Cost [kW]	2-norm Cost [kW^2]
1	Baseline	0	0
2	Heuristic	33.78	180180.18
3	Rule-based	1568.67	17645856.98
4	Hybrid	1082.01	18581054.32
5	Adaptive	37.72	83357.85

These results demonstrate that adaptive control not only improves frequency regulation and SoC management but also minimizes control effort, offering a favorable balance between operational performance and implementation complexity.

VII. CONCLUSION

This paper presented a comparative evaluation of five ESS control strategies for islanded microgrids using a QSTS-based framework. The adaptive controller sustained operation approximately 7% longer than the baseline while maintaining frequency limits with moderate control effort, demonstrating robust performance without reliance on forecasts. In contrast, heuristic and rule-based methods, though simple to implement, were less effective under dynamic conditions and required greater control effort. Overall, the results highlight a fundamental trade-off between implementation simplicity and operational resilience in ESS droop control, with adaptive strategies offering superior stability in renewable-oriented islanded microgrids.

Future work may extend the applicability of the proposed framework to larger and more complex islanded microgrids with higher renewable penetration. Evaluations under broader operating conditions and longer time horizons, together with joint consideration of ESS capacity planning, are expected to provide further insight into the scalability and long-term operational resilience of adaptive ESS droop control strategies. Interactions between power flow and control strategies, including convergence aspects, remain topics for future research.

REFERENCES

[1] S. Parhizi, H. Lotfi, A. Khodaei, and S. Bahramirad, "State of the art in research on microgrids: A review,"*IEEE Access*, vol. 3, pp. 890–925, 2015.
[2] G. Liu, "Microgrid Controller Survey Report: 2024 Update," Oak Ridge National Laboratory, Jan. 2024.
[3] D. J. Ryan, R. Razzaghi, H. D. Torresan, A. Karimi, and B. Bahrani, "Grid-supporting battery energy storage systems in islanded microgrids: A data-driven control approach," *IEEE Trans. Sustainable Energy*, vol. 12, no. 2, pp. 834–846, 2021.
[4] R. Kandari, N. Neeraj, and A. Micallef, "Review on Recent Strategies for Integrating Energy Storage Systems in Microgrids," *Energies*, vol. 16, 2023.
[5] N. M. Dehkordi, H. R. Baghaee, N. Sadati, and J. M. Guerrero, "Distributed noise-resilient secondary voltage and frequency control for islanded microgrids," *IEEE Trans. Smart Grid*, vol. 10, no. 4, pp. 3780–3790, 2019.
[6] C. Ma, J. Sun, J. Huang, and K. Wang, "Transient Stability Enhancement Strategy for Islanded Microgrids Based on Energy Storage–Virtual Synchronous Machine Control," *Energies*, vol. 16, no. 17, 2023.
[7] B. Li, Z. Hu, J. Li, and Y. Zhao, "A novel adaptive droop control strategy for SoC balance in PV-based DC microgrids," *Applied Energy*, vol. 335, 2023.
[8] V. C. Cunha, T. Kim, P. Siratarnsophon, N. Barry, S. Santoso, and W. Freitas, "Quasi-static time-series power flow solution for islanded and unbalanced three-phase microgrids," *IEEE Open Access J. Power Energy*, vol. 8, pp. 97–106, 2021.
[9] J. Rocabert, A. Luna, F. Blaabjerg, and P. Rodríguez, "Control of Power Converters in AC Microgrids," *IEEE Transactions on Power Electronics*, vol. 27, no. 11, pp. 4734-4749, Nov. 2012.
[10] F. Mumtaz, M. H. Syed, M. Al Hosani, and H. H. Zeineldin, *A Novel Approach to Solve Power Flow for Islanded Microgrids Using Modified Newton–Raphson With Droop Control of DG*, IEEE Trans. Sustainable Energy, vol. 7, no. 2, pp. 493–503, Apr. 2016.
[11] P. A. Ioannou and B. Fidan, *Adaptive Control Tutorial*. Philadelphia, PA, USA: SIAM, 2006.
[12] Y. A. R. I. Mohamed and E. El-Saadany, *Adaptive Decentralized Droop Controller to Preserve Power Sharing Stability of Paralleled Inverters in Distributed Generation Microgrids*, IEEE Trans. Power Electron., vol. 23, no. 6, pp. 2806–2816, Nov. 2008.
[13] Z. Guo, Z. Shuai, Y. Luo, *et al.*, "Adaptive least mean square controller for power quality enhancement in solar photovoltaic system," *Energies*, vol. 15, no. 23, pp. 8909, 2022.
[14] G. Tao, "Discrete-time adaptive state tracking control schemes using gradient algorithms," *Automatica*, vol. 169, Art. 111849, 2024.

979-8-3315-8138-1